Adsorption (2010) 16: 57–68
DOI 10.1007/s10450-010-9204-7

PROCEEDINGS OF PBAST5

Synthesis of carbon nanofibers from poly(ethylene glycol) with controlled structure

Yusuke Takahashi · Hirotaka Fujita · Wan-Hua Lin · Yuan-Yao Li · Takao Fujii · Akiyoshi Sakoda

Received: 30 June 2009 / Accepted: 13 January 2010 / Published online: 5 February 2010

Abstract Through fine tuning of synthesis conditions, we successfully synthesized three types of carbon nanofiber (CNF) (herring-bone carbon nanofiber, platelet carbon nanofiber, and cup-stacked carbon nanofiber) by the thermal decomposition of a mixture of poly(ethylene glycol) (PEG) and nickel chloride ($NiCl_2$). A series of experimental results demonstrated that the key factors for the selective synthesis of these CNFs were the (1) $NiCl_2$/PEG ratio, (2) drying time of the polymeric mixture, (3) state of PEG (liquid or solid) before temperature rising, and (4) temperature profile during the thermal decomposition. Changes in these conditions contributed to the formation of Ni catalyst particles from the catalyst $NiCl_2$ with different morphology, thereby resulting in the growth of different types of CNF or amorphous carbon products according to the catalyst particle's shape. Also, we found that the mechanism of CNF growth in this synthesis method was fundamentally the same as that in chemical vapor deposition (CVD).

Keywords Carbon nanofiber · Poly(ethylene glycol) · Thermal decomposition

Y. Takahashi (✉) · H. Fujita · T. Fujii · A. Sakoda
Department of Materials and Environmental Science, Institute of Industrial Science, the University of Tokyo, 4-6-1 Komaba Meguro-ku, Tokyo 153-8505, Japan
e-mail: ekusu@iis.u-tokyo.ac.jp

W.-H. Lin · Y.-Y. Li
Department of Chemical Engineering, Faculty of Engineering, National chung-cheng University, 168 University Road, Min Hsiung, Chia Yi 621, Taiwan, ROC

1 Introduction

Carbon nanofibers (CNFs) are among the most promising materials because of their unique structures and excellent features, which offer a variety of potential applications such as in fuel cells, lithium-ion batteries, chemical catalysis, adsorbents, and so on (Endo et al. 2004, 2006; Yoon et al. 2004; Yanagisawa et al. 2002; Zhao et al. 2007; van der Lee et al. 2005; Zhixin et al. 2007). The CNFs are categorized into the following four types primarily based on the graphene layer alignment to the fiber axis and whether the fiber has hollow core: (1) Platelet type, in which graphene layers are aligned at right angles to the fiber axis (Baker 1989), (2) Herring-bone type, in which graphene layers tilt at an angle to the fiber axis, (3) Tubular type, in which graphene layers are parallel to the fiber axis, and (4) Cup-stacked type, in which graphene layers tilt such as Herring-bone type (Yanagisawa et al. 2002). In addition, Tubular and Cup-stacked type have hollow core while Platelet and Herring-bone type are solid. And the structural difference inside the fibers provides each of these CNFs with different features; the tubular type is characterized by its high physicochemical stability and high electrical conductivity, like those of carbon nanotube (CNT), while the platelet type has a larger number of graphene edge sites on its surface as compared to the other three types, which indicates good chemical reactivity and adsorption characteristic of the platelet type (Yoon et al. 2005; Lim et al. 2004). These CNFs have been expected to exhibit their excellent abilities in different application fields. Taking their practical application into consideration, it is of great significance to establish a simple and useful technique for their selective synthesis.

Various synthesis methods of CNFs have been eagerly investigated for the past decade. Among them, chemical vapor

deposition (CVD) is the best-established method, capable of producing CNFs in large amounts as well as with a variety of graphene layer alignments (e.g., tubular type, cup-stacked type, herring-bone type, and platelet type). Typically, the CVD process is performed under hydrogen atmosphere using carbon monoxide or various kinds of gaseous hydrocarbons as carbon sources at temperatures ranging from 500 °C to 1200 °C. Many reports have revealed that the selective synthesis of these CNFs can be achieved through proper controls of morphology and dispersity of catalyst particles during the synthesis (Zheng et al. 2006; Huang and Li 2006; Saito 2005; Saito et al. 1998; Chen et al. 2005). In particular, the dispersity is a crucial factor for producing CNFs with high purity. Hence, a variety of catalyst synthesis methods such as the precipitation method, metal vapor vacuum arc (MEVVA) ion deposition, and on the like (Zhixin et al. 2007; Zheng et al. 2006) have been developed.

Recently, a novel method for synthesizing CNFs with ease and safety has been developed by Huang et al. (Huang and Li 2006). Using this method, one can synthesize platelet type CNF via the thermal decomposition of a mixture of poly (ethylene glycol) (PEG) and nickel chloride ($NiCl_2$) (Huang et al. 2006, 2008). The synthesis procedure mainly consists of three simple operations without any special techniques or tools: (1) synthesis of an aqueous solution of PEG so that PEG can serve as a carbon source and $NiCl_2$ can serve as a catalyst, (2) drying of the aqueous solution to obtain a PEG and $NiCl_2$ mixture without water, and (3) thermal decomposition of the dried mixture using a tubular furnace for the growth of CNFs. An advantage of this method is that it does not require the use of explosive and flammable hydrocarbon and hydrogen, commonly used in CVD. Furthermore, this method is unique in terms of its carbon source supply as well as catalyst synthesis, providing a possibility to develop novel CNFs with unique structure and characteristics. However, in the previous paper (Huang and Li 2006), this method was not systematically investigated and only the platelet type was obtained. Synthesizing the other three types of CNF is still a challenge. A second issue is that the mechanism of CNF synthesis is unclear in these earlier works. It was elucidated that thermal decomposition of the PEG and $NiCl_2$ mixture contributed to the formation of carbon-containing gases such as methane and carbon monoxide, which played an important role as carbon sources to produce the CNF; however, there has been no detailed investigation regarding the catalyst behavior during the synthesis. Also, though the $NiCl_2$/PEG ratio was proven to be an essential factor for the CNF synthesis (Huang et al. 2008), the reason for this has not yet been explained.

Hence, in this work, we made a systematic investigation of the relationship between synthesis conditions and the CNF types synthesized. We also examined the effect of several synthesis conditions on the morphology of the catalyst particles formed. The objectives of this work were:

(1) To establish the method for the selective synthesis of platelet, herring-bone, tubular, and cup-stacked CNFs, that is, for controlling graphene layer alignments with respect to the axis, and
(2) To elucidate the mechanisms of CNF synthesis in this method.

2 Experimental procedures

2.1 Synthesis

The standard procedure for CNF synthesis was as described previously (Huang and Li 2006). PEG (MW = 8000, melting point ≒ 60 °C) and $NiCl_2$ (purity >97%) were purchased from WAKO Chemicals, Japan. PEG was added to the aqueous solution of $NiCl_2$ and mixed well by a magnetic stirrer in a water bath at 60 °C for 30 min. The concentrations are described below. The 5 g of mixed solution was uniformly spread on the upper surface of a silicon wafer which is 3 cm wide and 10 cm long, followed by drying on a hot plate at 70 °C. The dried mixture of PEG and $NiCl_2$ on the silicon wafer was then solidified at ambient temperature. Subsequently, the mixture on the silicon wafer was placed in a tubular furnace (inner diameter: 5 cm, length of hot-zone: 85 cm) and, after nitrogen purge (500 sccm, 30 min), heated to 750 °C for the thermal decomposition of the mixture and thereby the growth of CNFs.

The operation conditions in this work involved the (a) PEG/$NiCl_2$ ratio, (b) drying time of the aqueous solution, and (c) temperature increase rate during the thermal decomposition of the solidified mixture. The same amount of PEG and water were mixed and the scheduled amount of $NiCl_2$ was added. The mass ratio of PEG/$NiCl_2$ was changed ranging from 10 to 1500, and the aqueous solution without containing $NiCl_2$ was also examined. The drying time was changed in a range from 0 to 96 hours. During the thermal decomposition, the temperatures were controlled according to temperature program (A) or (B), in which a relatively slow or quick temperature rise took place, respectively. In program (A), the temperature was increased via three steps to 750 °C. First, the temperature was elevated from ambient temperature to 400 °C and kept constant for 1 hr. Second, it was further elevated to 500 °C and again kept constant for 1 hr. Third, it was elevated to 750 °C and kept constant for 1 hr. At each step, the rate of temperature rise was 15 °C/min. Meanwhile, in program (B), the temperature was elevated in one step to 750 °C at a rate of 60 °C/min and kept constant for 1 hr.

2.2 Characterization

To analyze the structure of CNFs, we observed the synthesized CNF samples by field emission scanning electron mi-

croscope (FE-SEM) (Hitachi S-4500) and transmission electron microscope (TEM) (JEM-2000EXII).

Also, to analyze the morphology and dispersity of Ni particles in the solidified mixture, we cut the solidified mixture into small pieces approximately 0.5 mm thick and performed the gold deposition treatment by vacuum deposition, prior to the observation by FE-SEM.

Moreover, purity of synthesized CNFs, the percentage of desired type of CNF in the sample, was approximately calculated by visual judgment of area ratio between the CNF and amorphous carbon as impurity.

3 Result and discussion

3.1 Carbon products synthesized

As shown in Figs. 1 to 3, three types of CNFs (platelet type, cup-stacked type, and herring-bone type) were successfully synthesized through fine tuning of synthesis conditions. To the best of our knowledge, this is the first report on the synthesis of cup-stacked and herring-bone type CNFs via this method. We were not able to synthesize the tubular type of CNF under any conditions employed in this work. We were able to obtain amorphous carbon agglomerates with Ni particles with a diameter of approximately 1 µm and amorphous film covering the surface of a silicon wafer, as shown in Figs. 4 and 5, respectively.

The features of CNFs obtained in this work are summarized as follows. The platelet CNF was approximately 40 to 50 nm in diameter and 2 to 5 µm long, as shown in Fig. 1. It is worth noting that the platelet CNF obtained by this method has a relatively small diameter in comparison to those obtained by CVD methods, as pointed out by Huang et al. (Huang and Li 2006), indicating one of the advantages of this synthesis method. As mentioned previously, the platelet type is strongly characterized by a large number of graphene edge sites on its surface, to which a variety of functional groups can be bound for the sake of surface modification (Zhao et al. 2007; Zhixin et al. 2007). The smaller diameter leads to a larger number of edge sites per unit weight of the fiber, suggesting that the platelet type fabricated by this method might have wider applications. Differing from the results obtained in this work, the platel et type CNF synthesized by Huang et al. was 20 nm in diameter (Huang and

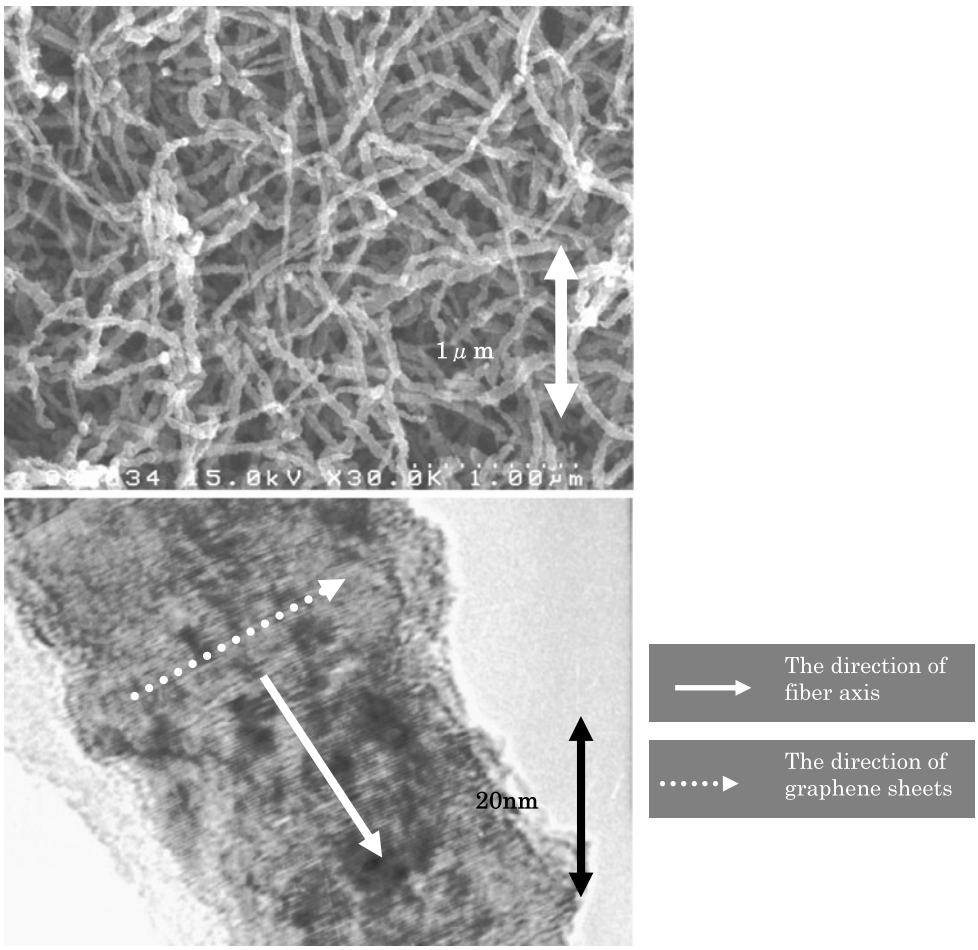

Fig. 1 SEM and TEM images of platelet CNF

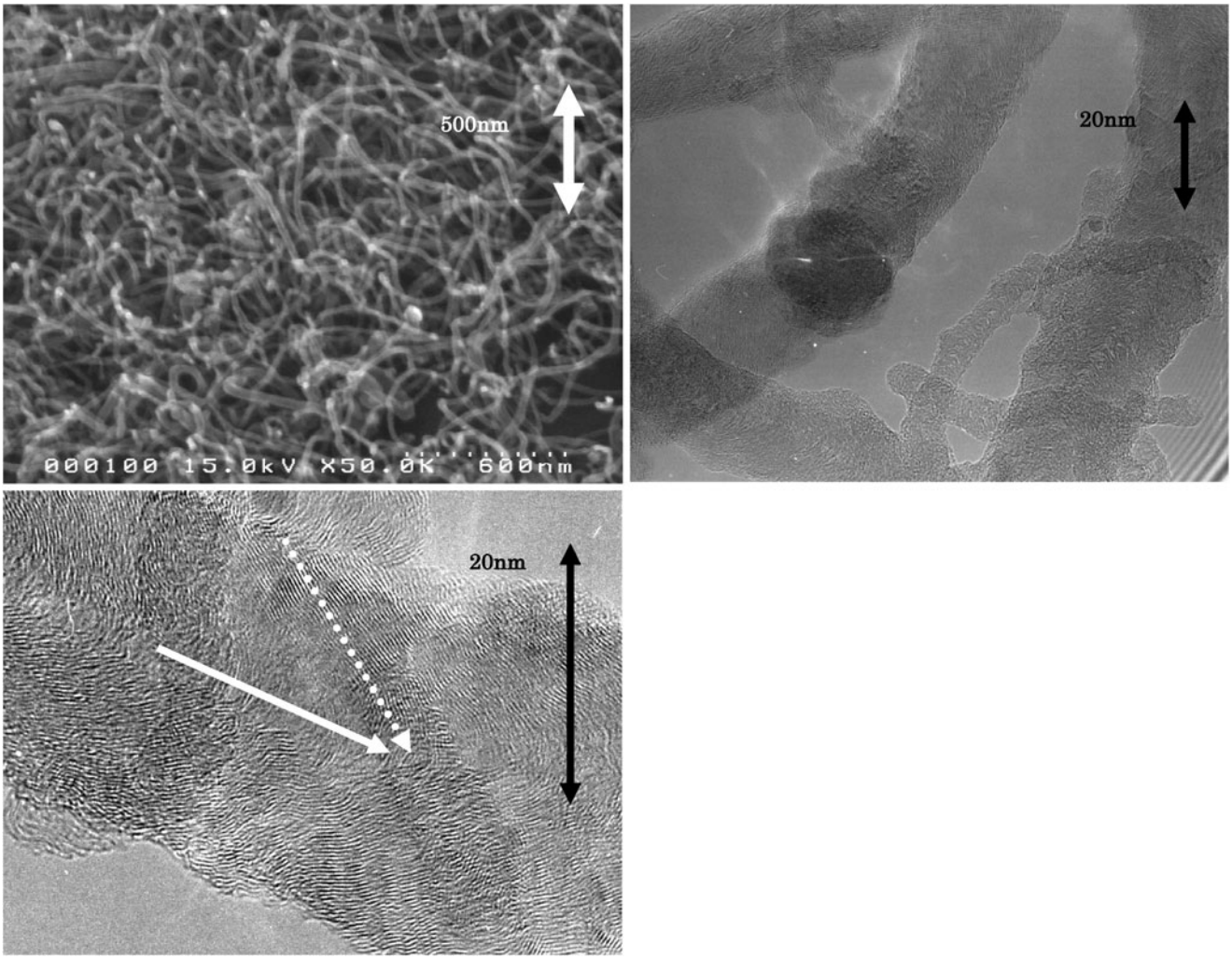

Fig. 2 SEM and TEM images of herring-bone CNF

Li 2006), which raised the possibility that further investigation of synthetic conditions might result in more precise control over the diameter via this method. The herring-bone type synthesized CNF was approximately 40 nm in diameter and 5–10 µm long, as shown in Fig. 2. Meanwhile, the cup-stacked type synthesized was approximately 30 nm in diameter and 10–20 µm long, as shown in Fig. 3. These two types of CNFs synthesized in this work were very similar to those synthesized by conventional CVD methods in terms of the fiber diameter and length.

3.2 Effect of synthesis conditions on carbon products

Figures 6 to 8 show the relationship between synthesis conditions and carbon products synthesized. Figure 9-(A) to (E) show the SEM or TEM images of Ni particles in the carbon products. The types of CNF were strongly and regularly affected by the PEG/$NiCl_2$ ratio, drying time, and temperature profile during the thermal decomposition.

The PEG/$NiCl_2$ ratio must be set at a proper range for the synthesis of the CNFs, as previously pointed out by Huang et al. (Huang et al. 2006). Small ratios resulted in the predominant formation of amorphous carbon agglomerates, and similar results are found in the literature. This formation was likely related to the behavior of Ni particles serving as catalysts, because proper control over the particles size and morphology was essential for the growth of CNFs (Rodriguez et al. 1995; Monthioux et al. 2007). Figure 9-(A) shows a SEM image of Ni particles in the amorphous carbon agglomerates. Considerably larger particles (>500 nm) were observed as compared with those in the CNFs (30–50 nm), indicating that an excess of $NiCl_2$ led to excessive aggregation during the synthesis and thereby to the formation of Ni particles too large to catalyze the growth of CNF. Meanwhile, excessively large ratios led to the formation of amorphous carbon film. The amorphous carbon film was also produced even at the PEG/$NiCl_2$ ratio of infinity, that is, in the absence of $NiCl_2$, meaning that its formation took place

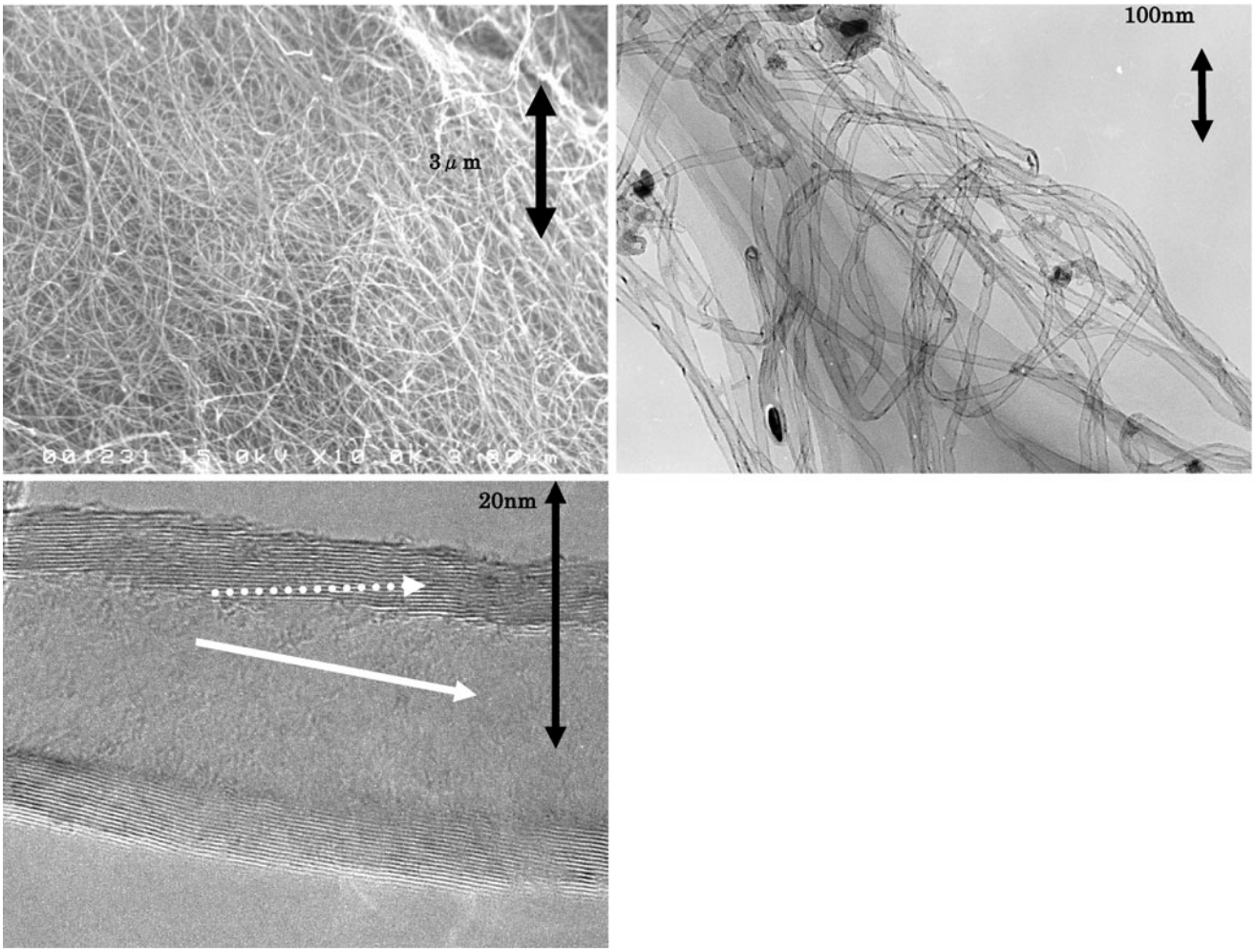

Fig. 3 SEM and TEM images of cup-stacked CNF

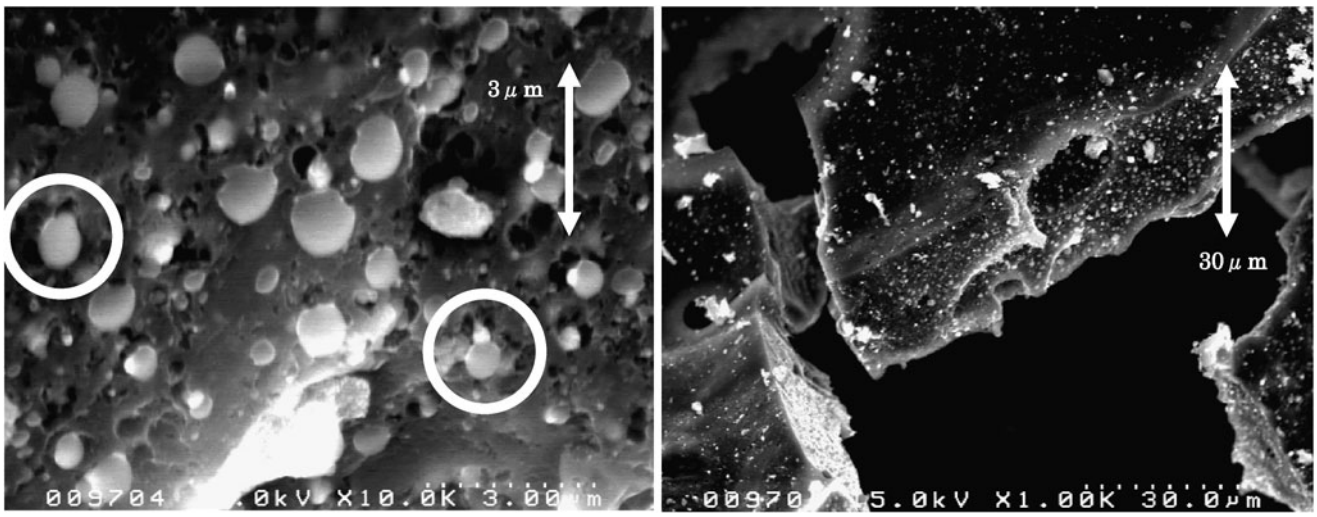

Fig. 4 SEM images of amorphous agglomerates. Typical Ni particles are highlighted with *open circles*

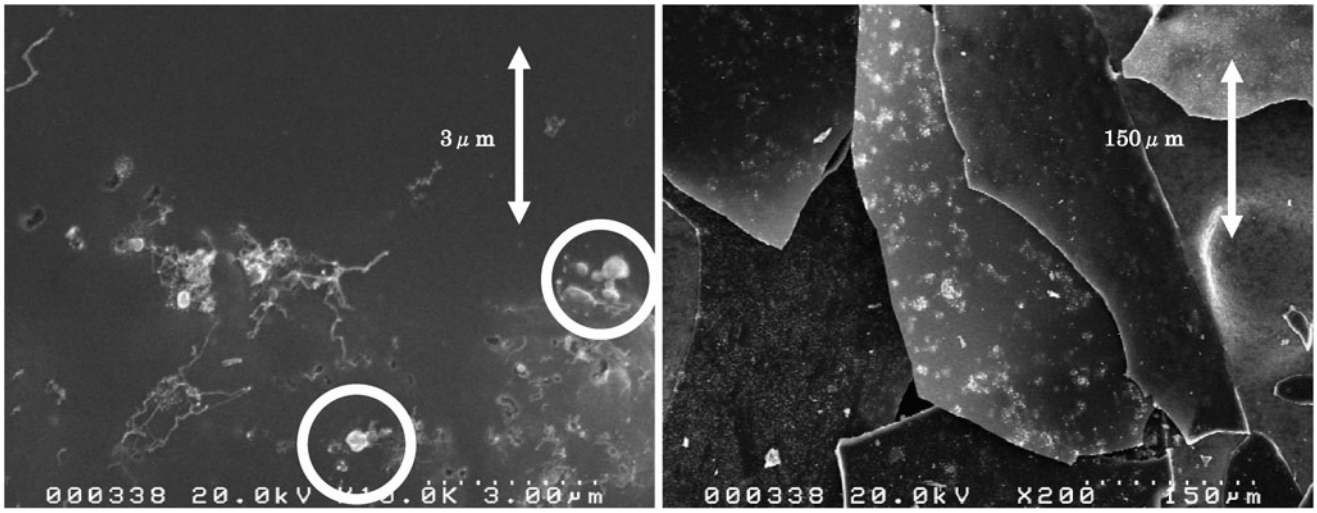

Fig. 5 SEM images of amorphous carbon film. Typical Ni particles are highlighted with *open circles*

Fig. 6 Carbon products synthesized in the temperature profile of program (A) (low temperature rising rate (15 °C/min), starting from solid PEG)

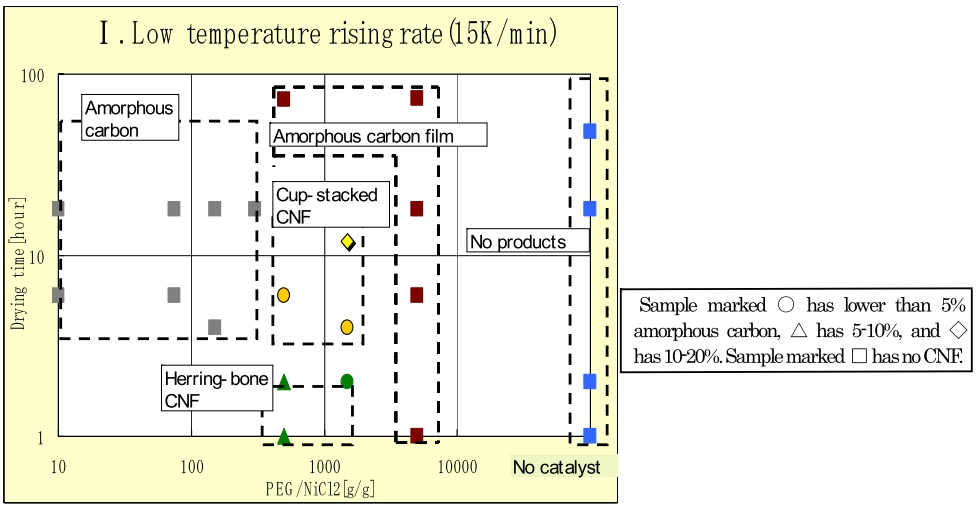

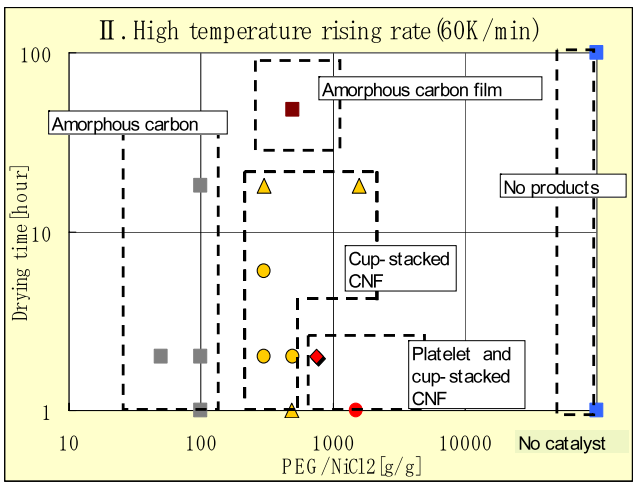

Fig. 7 Carbon products synthesized in the temperature profile of program (B) (high temperature rising rate (60 °C/min), starting from solid PEG)

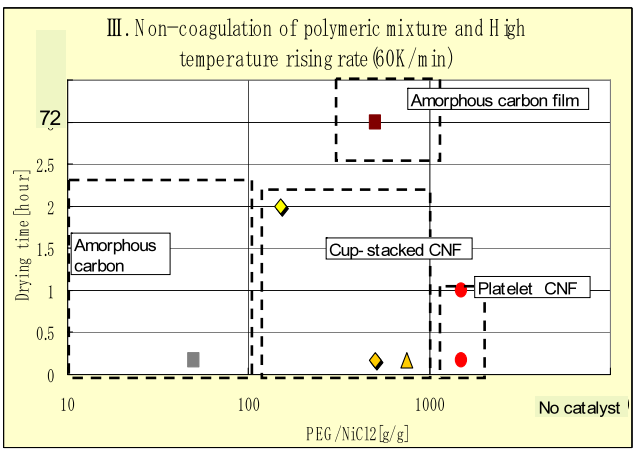

Fig. 8 Carbon products synthesized in the temperature profile of program (B) (high temperature rising rate (60 °C/min), starting from liquid PEG)

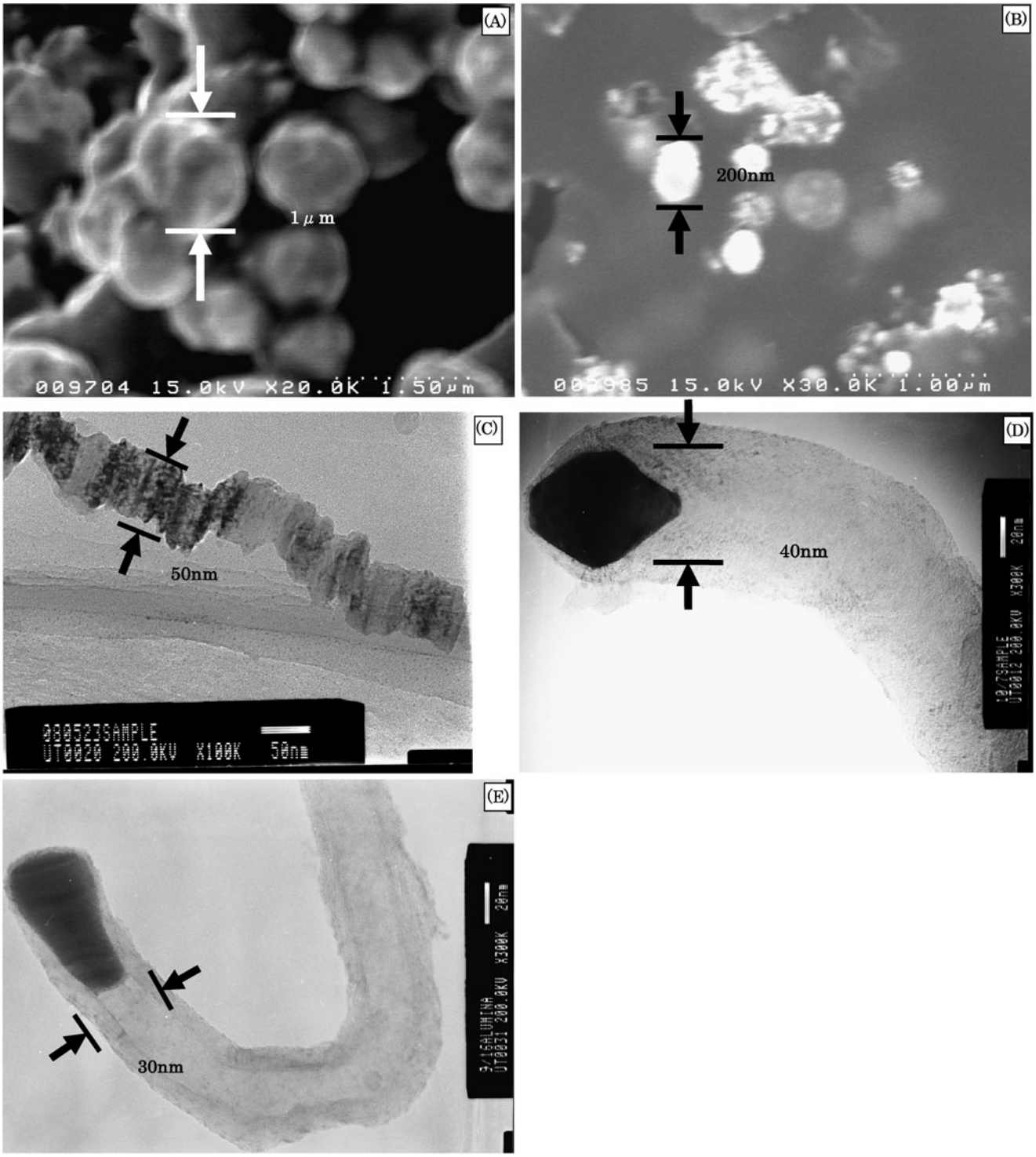

Fig. 9 SEM images of Ni particles in (**A**) amorphous carbon (**B**) amorphous carbon film and TEM images of Ni particles in (**C**) platelet CNF, (**D**) herring-bone CNF and (**E**) cup-stacked CNF. Experimental conditions of (**A**) are (PEG:$NiCl_2$ = 10:1. Dried for 20 h at 70 °C. Solidified before temperature rising. Temperature program (A)); Experimental conditions of (**B**) are (PEG:$NiCl_2$ = 500:1. Dried for 72 h at 70 °C. Solidified before temperature rising. Temperature program (A)); Experimental conditions of (**C**) are (PEG:$NiCl_2$ = 1500:1. Dried for 1 h at 70 °C. Not solidified before temperature rising. Temperature program (B)); Experimental conditions of (**D**) are (PEG:$NiCl_2$ = 1500:1. Dried for 1 h at 70 °C. Solidified before temperature rising. Temperature program (A)); Experimental conditions of (**E**) are (PEG:$NiCl_2$ = 500:1. Dried for 6 h at 70 °C. Solidified before temperature rising. Temperature program (A))

when $NiCl_2$ was absolutely inactive as a catalyst. The excessively low concentrations of $NiCl_2$ possibly resulted in insufficient formation of the catalyst particles.

The range of the PEG/$NiCl_2$ ratio required for the CNF growth was likely to change as the temperature profile was varied during the thermal decomposition. However, we found that a ratio ranging from 150 to 1500 was necessary for CNF growth under the conditions employed in this work. The drying time was also a key factor for CNF growth. Excessively long drying led to the formation of an amorphous carbon film. At above 3 hrs of drying time, the longer the drying was, the higher the ratio of amorphous carbon film in the products. At above 72 hrs, carbon film formation completely predominated, because the Ni particles aggregated in PEG into extremely large particles with diameters of approximately 200 nm, as shown in Fig. 9-(B), resulting in the complete inactivation of the catalyst. At excessively short drying times, insufficient water vaporization occurred. To produce CNF, we had to use a drying time ranging from 1 to 3 hrs. These results suggested that the catalyst energetically preferred to aggregate in PEG into micrometer-sized particles. However, we suspected that PEG serving as a solvent can delay the aggregation due to its high viscosity and thus contribute to the formation of Ni particles with proper size and dispersity for CNF formation. Figure 10 shows the SEM image of Ni particles in the solidified mixture synthesized under the synthesis condition in which the cup-stacked type CNF was produced. This shows the formation of nanometer-sized $NiCl_2$ particles in solidified PEG. The changes in temperature profile during the thermal decomposition provided a drastic change in carbon products, as shown in Figs. 6 and 7. The CNFs obtained were platelet and cup-stacked types in temperature program (B), while they were cup-stacked and herring-bone types in program (A).

Proper combinations of PEG/$NiCl_2$ ratio, drying time, and temperature profile allowed the high-purity synthesis of cup-stacked and herring-bone type CNFs, as shown in Fig. 6. High-purity synthesis of platelet type CNF was not achieved, despite the fine tuning of these three sets of conditions. The platelet type was produced at any case with coexistence of the cup-stacked type. On the other hand, the cup-stacked type with high purity could be obtained under a broader range of synthesis conditions as compared to the other CNFs. To obtain the high-purity synthesis of platelet type CNF, the solidification of PEG must not occur prior to the thermal decomposition. Actually, the types of CNF synthesized were only slightly affected by the state of PEG (liquid or solid) before the temperature was raised, as shown in Figs. 7 and 8. However, the purity of CNFs synthesized was significantly influenced by the PEG state. When the aqueous solution was solidified before the temperature was raised, synthesized platelet

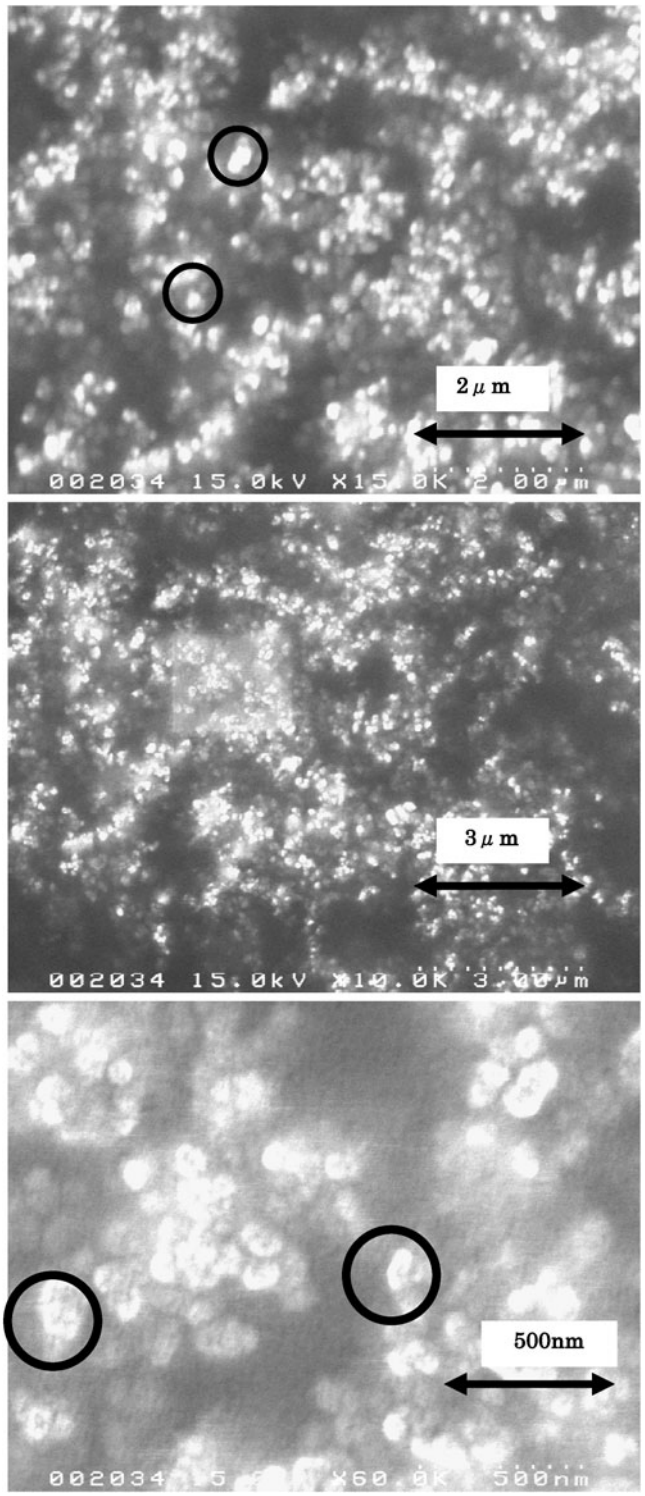

Fig. 10 SEM images of $NiCl_2$ particle in PEG and $NiCl_2$ mixtures. PEG:$NiCl_2$ = 500:1. Dried for 1 h at 70 °C. Solidified at room temperature. Typical Ni particles are highlighted with *open circles*

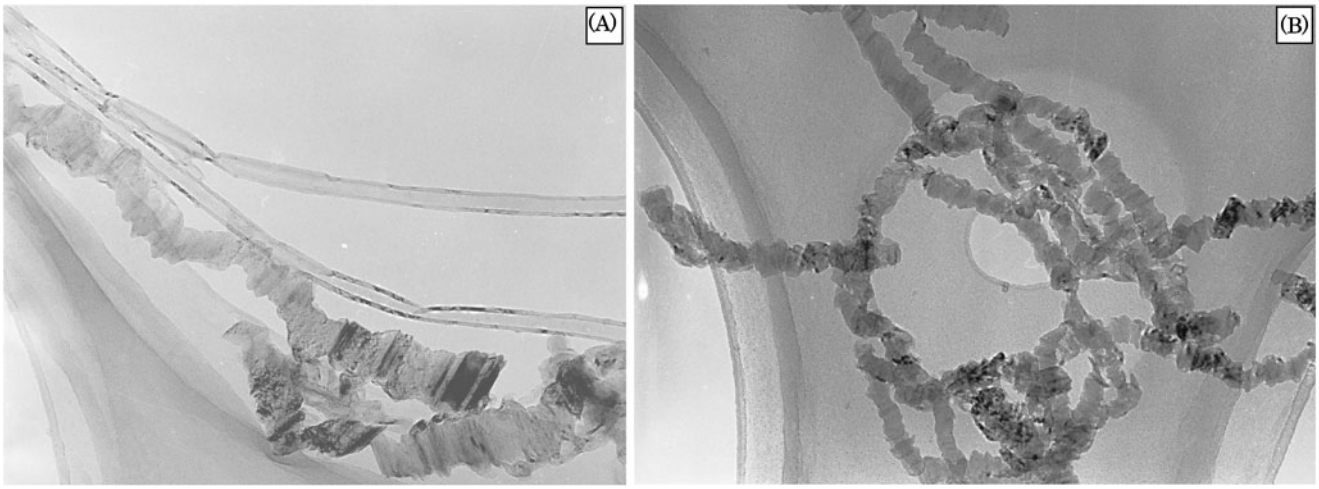

Fig. 11 TEM images of (**A**) the mixture of platelet and cup-stacked CNF (PEG:$NiCl_2$ = 1500:1. Solidified before temperature rising (program (B)), and (**B**) platelet CNF (PEG:$NiCl_2$ = 1500:1. Not solidified before temperature rising (program (B))

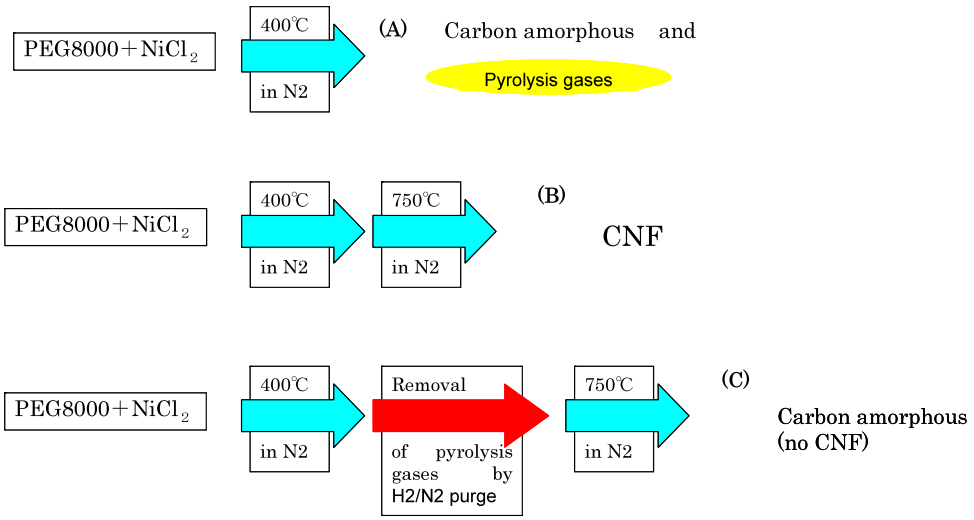

Fig. 12 Schematic diagram of the experiments about CNF growth mechanism. Other experimental conditions are (PEG:$NiCl_2$ = 500:1. Dried for 3 h at 70 °C. Solidified before temperature rising)

CNF was mixed with cup-stacked type CNF, as shown in Fig. 11-(A). The high-purity synthesis of platelet type CNF was achieved only when the solidification of PEG did not occur before the temperature was raised, as shown in Fig. 11-(B).

3.3 Mechanism of CNF synthesis

The vapor–liquid–solid growth is generally accepted as a CNT/CNF growth mechanism in the CVD, in which the carbon source diffuses and dissolves into the catalyst, followed by the formation of graphene layers on the catalyst surface due to the precipitation of supersaturated carbon (Saito 2005; Saito et al. 1998; Baker 1989; Madronero 1995). Also, the deformation of the catalyst during the growth of graphene layers plays a crucial role in producing the CNFs with a variety of graphene layer alignments (Monthioux et al. 2007), because the graphene layer is formed while mimicking the interfaces of catalyst particles (Zheng et al. 2006; Rodriguez et al. 1995). Zheng et al. obtained platelet CNF from granular thin catalyst flakes (several tens of nanometers thick and 100–300 nm wide).

The mechanism of selective synthesis in the method employed in this work is also explained to a certain degree in terms of the size and morphology of the catalyst particle formed. The relationship between the catalyst morphology and resultant CNF types can be summarized as follows from the experimental results, as shown in Fig. 9:

- When the catalyst particle was approximately 50 nm in diameter and plate-like in morphology, the formation of platelet type CNF took place.
- When the catalyst particle was approximately 40 nm in diameter and rhomboid in morphology, the formation of herring-bone type CNF took place.

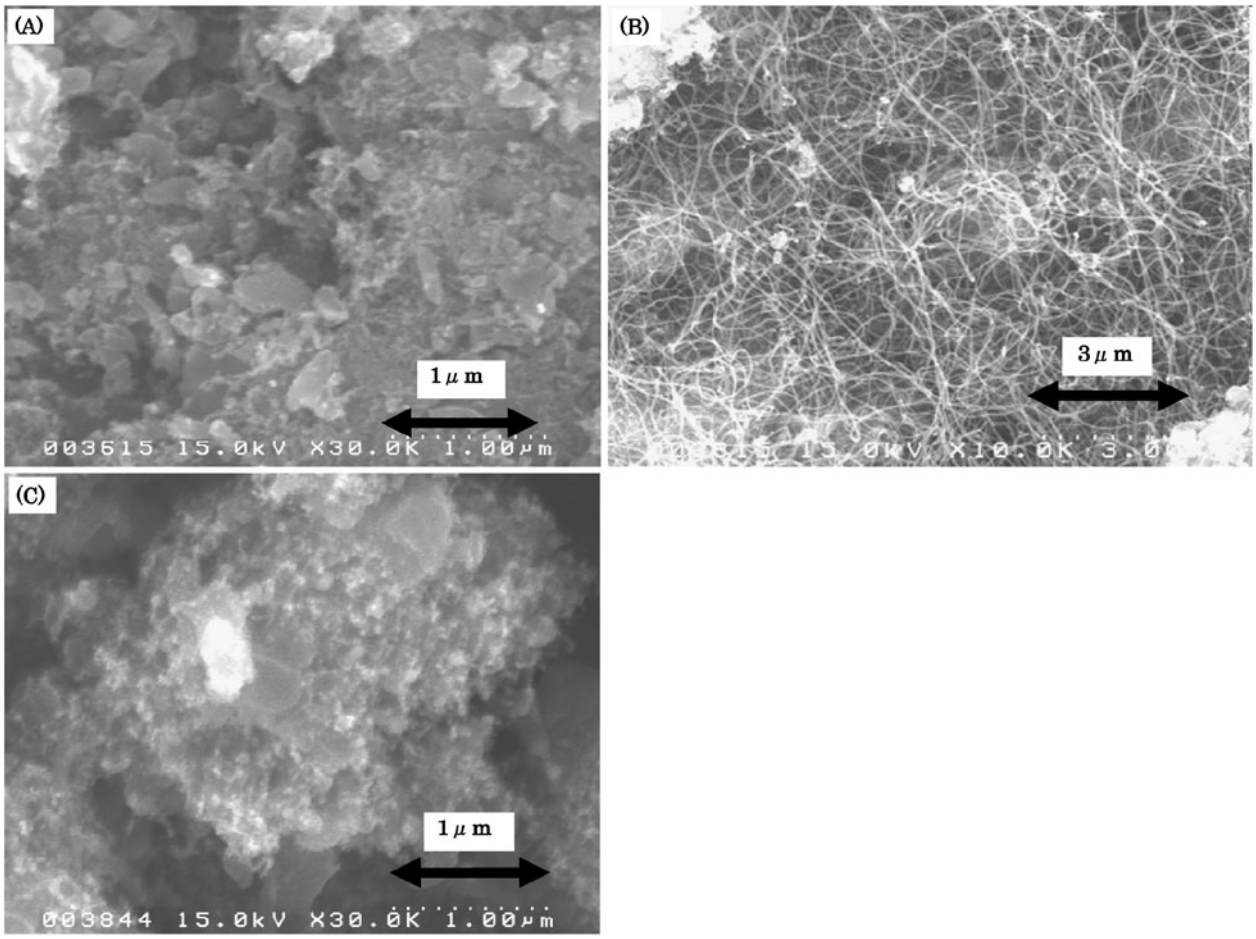

Fig. 13 SEM images about Fig. 12. (**A**) is amorphous carbon grown during the 400 °C heating, (**B**) is the cup-stacked CNF sample heated at 750 °C with pyrolysis gases of PEG, and (**C**) is the sample heated at 750 °C in H_2/N_2 atmosphere

- When the catalyst particle was approximately 30 nm in diameter and truncated-cone in morphology, the formation of cup-stacked type CNF took place.

Similar results can be found in the literature (Monthioux et al. 2007). Despite slight differences in catalyst morphology, they were able to control the selective synthesis of three CNFs by the catalyst size and morphology using a CVD method.

In this paper, the formation mechanism was investigated by several experiments. When PEG/$NiCl_2$ was thermally decomposed at 400 °C, it changed pyrolysis gases such as CO, CH_4, H_2, and etc. (Huang and Li 2006) leaving solid amorphous carbon as shown in Fig. 13-(A). Our experimental results clarified that if the pyrolysis gases were removed by H_2/N_2 flow (volume ratio: 1/10), CNF didn't grow on the amorphous carbon (Fig. 13-(C)) after heating at 750 °C. On the other hand, CNF was grown when the sample was heated with the pyrolysis gases at 750 °C (Fig. 13-(B)). This indicates, like conventional CVD, the CNF growth in the method requires gaseous carbon source such as CO and CH_4 derived from PEG decomposition.

Then, we suggest that the formation mechanism of CNF by the method we employed in the present work was basically the same as that occurring as a result of using the conventional CVD methods.

In summary, the conditions such as PEG/$NiCl_2$ ratio, drying time, and temperature profile governed not only the catalyst morphology but also the resultant CNF types. However, how these factors influenced the catalyst morphology remains unclear. Further studies are needed to gain a better understanding of catalyst behavior and CNF growth during the synthesis.

The possible mechanism of Ni particles synthesis and CNF synthesis is summarized in Fig. 14 and includes the following steps:

(1) PEG and $NiCl_2$ are dissolved in an aqueous solution.
(2) Drying on a hotplate gradually vaporizes the water in the solution, forming Ni particles dispersed in PEG due to its supersaturation. The aggregation of Ni particles

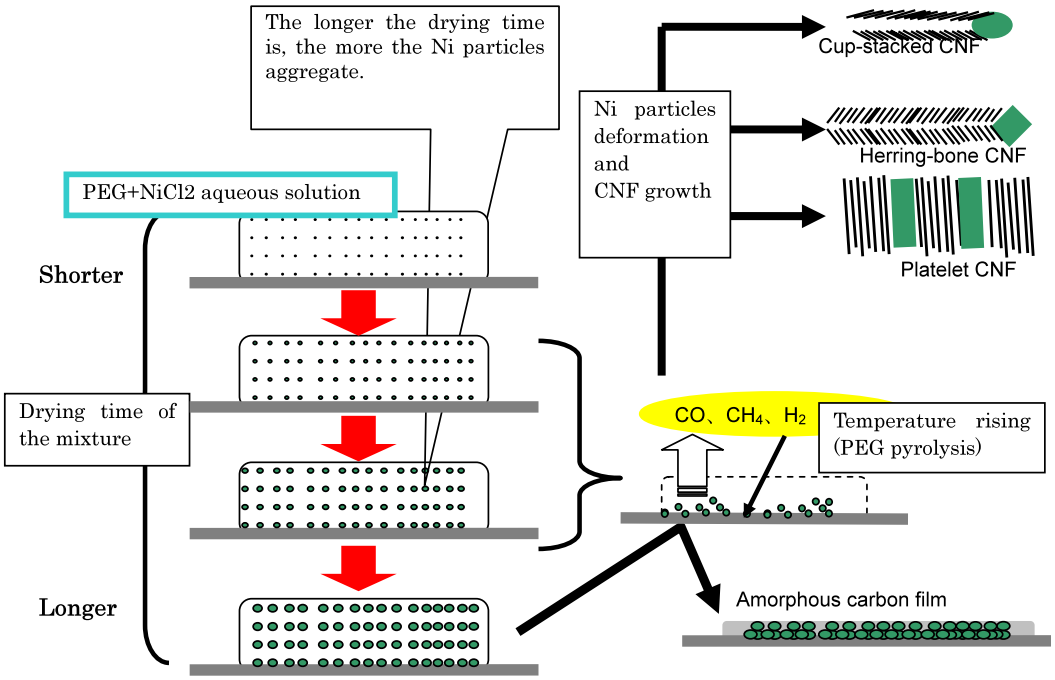

Fig. 14 Schematic diagram of the mechanism of Ni particles synthesis and CNF synthesis

proceeds with increasing drying time. Proper drying allows the formation of Ni particles with the proper size and dispersity for the growth of CNF. Excessively long drying leads to excessive aggregation, resulting in the production of an amorphous carbon film.

(3) Carbon-containing gas serving as a carbon source is generated during the thermal decomposition of PEG. The carbon sources diffuse into the Ni particles, followed by the formation of graphene planes on the catalyst surface due to the precipitation of the supersaturated carbon. The deformation of the Ni particles takes place during the formation of the graphene layer. The resultant catalyst morphologies are categorized into three types: (1) plate-like morphology from which the platelet type CNF grows, (2) rhombic morphology from which the herring-bone type CNF grows, and (3) truncated-cone morphology, from which the cup-stacked type CNF grows. The synthesis conditions such as PEG/$NiCl_2$ ratio, drying time, state of PEG (liquid or solid) before temperature rising, and temperature profile during the thermal decomposition determine the morphology of the catalyst particles, meaning that these conditions are dominant factors for the selective synthesis of the CNFs.

4 Conclusions

(1) Through the fine tuning of synthesis conditions, three types of carbon nanofibers (herring-bone carbon nanofiber, platelet carbon nanofiber, and cup-stacked carbon nanofiber) were successfully synthesized by the thermal decomposition of a mixture of poly(ethylene glycol) (PEG) and nickel chloride ($NiCl_2$). Tubular type CNF was not obtained under any conditions employed in this work. A series of experimental results showed that the key factors for the selective synthesis of these CNFs were the (1) $NiCl_2$/PEG ratio, (2) drying time, (3) state of PEG (liquid or solid) before the temperature was raised, and (4) temperature profile during the thermal decomposition. Proper combinations of the PEG/$NiCl_2$ ratio, drying time, and temperature profile allowed the high-purity synthesis of three types of CNF.

(2) The mechanism of selective synthesis in the method employed in this work is explained to a certain degree in terms of the size and morphology of the catalyst particles formed. Changes in the above synthesis conditions contributed to the formation of Ni particles of varying morphology and size, thereby resulting in the growth of different types of CNF. This fact agreed with the mechanism of selective synthesis by the conventional CVD methods, suggesting that the formation mechanism of CNF by our method was basically the same as that occurring during use of the conventional CVD methods.

(3) The selective and high-purity synthesis of the platelet CNF was demonstrated on the basis of the new findings described above.

References

Baker, R.T.K.: Catalytic growth of carbon filaments. Carbon **27**(3), 315–323 (1989)

Chen, D., et al.: Synthesis of carbon nanofibers: effects of Ni crystal size during methane decomposition. J. Catal. **229**, 82–96 (2005)

Endo, M., et al.: Nanocarbon. Senni-to-Kougyou **60**(6), 260–265 (2004) (in Japanese)

Endo, M., et al.: Development and application of carbon nanotubes. Jpn. J. Appl. Phys. **45**(6A), 4883–4892 (2006)

Huang, C.H., Li, Y.Y.: In situ synthesis of platelet graphite nanofibers from thermal decomposition of poly(ethylene glycol). J. Phys. Chem. B **110**(46), 23242–23246 (2006)

Huang, C.H., et al.: Synthesis of carbon nanofibres from a liquid solution containing both catalyst and polyethylene glycol. Nanotechnology **17**, 4629–4634 (2006)

Huang, C.H., et al.: Synthesis and characterization of porous carbon nanofibers from thermal decomposition of poly(ethylene glycol). J. Phys. Chem. C **112**, 926–931 (2008)

Lim, S., Yoon, S.H., et al.: Surface modification of carbon nanofiber with high degree of graphitization. J. Phys. Chem. B **108**, 1533–1536 (2004)

Madronero, A.: Possibilities for the vapour-liquid-solid model in the vapour-grown carbon fibre growth process. J. Mater. Sci. **30**, 2061–2066 (1995)

Monthioux, M., et al.: Texturising and structurising mechanisms of carbon nanofilaments during growth. J. Mater. Chem. **17**, 4611–4618 (2007)

Rodriguez, N.M., et al.: Catalytic engineering of carbon nanostructures. Langmuir **11**, 3862–3866 (1995)

Saito, Y.: In Introduction to Material Science for Carbon Nanotube. Korona-sya (2005) (in Japanese)

Saito, Y., et al.: In Fundamentals of Carbon Nanotube. Korona-sya (1998). (in Japanese)

van der Lee, M.K., et al.: Deposition precipitation for the synthesis of carbon nanofiber supported nickel catalysts. J. Am. Chem. Soc. **127**, 13573–13582 (2005)

Yanagisawa, T., et al.: Structure and basic properties of cup-stacked type carbon nanofiber. Mol. Cryst. Liq. Cryst. **387**, 167–171 (2002)

Yoon, S.H., et al.: Novel carbon nanofibers of high graphitization as anodic materials for lithium ion secondary batteries. Carbon **42**, 21–32 (2004)

Yoon, S.H., et al.: A conceptual model for the structure of catalytically grown carbon nano-fibers. Carbon **43**, 1828–1838 (2005)

Zhao, T.J., et al.: The effect of graphitic platelet orientation on the properties of carbon nanofiber supported Pd catalysts synthesized by ion exchange. Top. Catal. **45**(1–4), 87–91 (2007)

Zheng, R., et al.: Synthesis, characterization, and growth mechanism of platelet carbon nanofibers. Carbon **44**, 742–746 (2006)

Zhixin, Y., et al.: Role of surface oxygen in the synthesis and deactivation of carbon nanofiber supported cobalt Fischer-Tropsch catalysts. Top. Catal. **45**, 1–4 (2007)